Vol. 45 (2014) *ACTA PHYSICA POLONICA B* No 5

MEASUREMENT OF STRONG COUPLING CONSTANT BY USING EVENT SHAPE MOMENTS IN PERTURBATIVE THEORY*

L. Khajooee, T. Kalalian, R. Saleh-Moghaddam
A. Sepehri, M.E. Zomorrodian

Department of Physics, Faculty of Sciences, Ferdowsi University of Mashhad
91775-1436, Mashhad, Iran

(Received December 19, 2012; revised version February 3, 2014; final version received March 12, 2014)

We measure the strong coupling constant at NNLO corrections. We do this analysis with moments of event shape variables: thrust, C parameter, heavy hemisphere mass, wide and total jet broadening, by fitting the L3 and DELPHI data with NNLO model. Our real data are consistent with NNLO calculations, because the analysis involves higher order terms in QCD calculations.

DOI:10.5506/APhysPolB.45.1077
PACS numbers: 13.66.Bc, 11.15.Me, 12.38.Bx

1. Introduction

Analyses of events originating from e^+e^- annihilation into hadrons allow for studies [1–6] of Quantum Chromo Dynamics (QCD), the theory of the strong interaction [7–12]. The comparison of observables such as jet production rates or event shapes with theoretical predictions provides access to the determination of the strong coupling ($\alpha_{\rm s}$). Recently, significant progress in the theoretical calculations of event shape moments and three jet rates has been made [13].

Event shape variables are interesting for studying the interplay between perturbative and non-perturbative dynamics. Apart from distributions of these observables one can study mean values and higher moments. The $n^{\rm th}$

moment of an event shape observable Y is defined by [14]

$$\langle y^n \rangle = \frac{1}{\sigma_{\text{had}}} \int\limits_0^{y_{\max}} y^n \frac{d\sigma}{dy} dy \,, \tag{1}$$

where $y_{\max}$ is the kinematically allowed upper limit of the observable.

Measurements of the strong coupling (α_{s}) of QCD, the theory of strong interaction, using different observables and different analysis methods serve as an important consistency test of QCD.

In Section 2, we perform a new extraction of α_{s} from L3 and DELPHI data with Next-to-Next-to-Leading Order (NNLO) model and measure the strong coupling constant at NNLO then we compare the moment observables with other experiments. The last section includes our conclusions.

2. NNLO corrections to event shape moments in electron positron annihilation

2.1. Definition of the observables

The properties of hadronic events may be characterized by a set of event shape observables. In this subsection, we briefly recall the definitions of the relevant event shape observables. The event shape variables are defined by the following sentences.

2.1.1. Thrust (T)

Thrust (T) defined by the expression [15–18]:

$$T = \max \left(\frac{\sum_i \left| \vec{P}_i \vec{n} \right|}{\sum_i |p_i|} \right) . \tag{2}$$

The thrust axis $\vec{n}_{\text{T}}$ is the direction $\vec{n}$ which maximizes the expression in parentheses the value of the thrust can vary between 0.5 and 1.

A plane through the origin and perpendicular to $\vec{n}_{\text{T}}$ divides the event into two hemispheres H_1 and H_2.

2.1.2. C-Parameter

The linearised momentum tensor θ^{ij} is defined by [19, 20]

$$\theta^{ij} = \frac{1}{\sum_1 \left| \vec{P}_{\text{L}} \right|} \sum_k \frac{P_k^i P_k^i}{\left| \vec{P}_k \right|} \,, \qquad i,j = 1,2,3 \,, \tag{3}$$

where the sum runs over all final state particles and P_k^i is the i^{th} component of the three-momentum $\vec{P}_k$ of particle k in the centre-of-mass system. The tensor θ is normalized to have unit trace. In terms of the eigenvalues of the θ tensor, λ_1, λ_2, λ_3, with $\lambda_1 + \lambda_2 + \lambda_3 = 1$, one defines

$$C = 3(\lambda_1\lambda_2 + \lambda_2\lambda_3 + \lambda_3\lambda_1)\,. \tag{4}$$

The C-parameter exhibits in perturbation theory a singularity at the three-parton boundary $c = \frac{3}{4}$.

2.1.3. Heavy hemisphere mass (ρ)

The hemisphere masses are defined by [21]

$$M_i^2 = \left(\begin{array}{c}\sum Pj \\ j \in H_i\end{array}\right)^2, \qquad i = 1, 2\,, \tag{5}$$

where P_j denotes the four-momentum of particle j. The heavy hemisphere mass M_{H} is then defined by

$$M_{\mathrm{H}}^2 = \max\left(M_1^2, M_2^2\right)\,. \tag{6}$$

It is convenient to introduce the dimensionless quantity

$$\rho = \frac{M_{\mathrm{H}}^2}{Q^2}\,, \tag{7}$$

where Q is the centre-of-mass energy. In the leading order, the distribution of the heavy hemisphere mass (ρ) is identical to the distribution of $(1 - T)$.

2.1.4. Jet broadening observables B_{T} and B_{W}

The hemisphere broadening [22–26] are defined by

$$B_K = \left(\frac{\sum_{i \in H_K} |\vec{p}_i \times \vec{n}_{\mathrm{T}}|}{2\sum_i |\vec{p}_i|}\right)\,. \tag{8}$$

For each of the two event hemispheres, H_K defined above. The two observables are defined by

$$B_{\mathrm{T}} = B_1 + B_2 \qquad \text{and} \qquad B_{\mathrm{W}} = \max\left(B_1, B_2\right)\,, \tag{9}$$

where B_{T} is the total and B_{W} is the wide-jet broadening.

2.2. Theoretical framework

The perturbative QCD expansion for the moment of the event shape observable y up to NNLO at centre-of-mass energy $\sqrt{S}$ for renormalization scale $\mu^2 = s$ and $\alpha_s \equiv \alpha_s(S)$ is given by [14]

$$\langle y^n\rangle \left(s,\mu^2=s\right) = \left(\frac{\alpha_s}{2\pi}\right)^1 \overline{A}_{y,n} + \left(\frac{\alpha_s}{2\pi}\right)^2 \overline{B}_{y,n} + \left(\frac{\alpha_s}{2\pi}\right)^3 \overline{C}_{y,n} + O\left(\alpha_s\right)^4 . \quad (10)$$

The detailed calculations of the coefficients $A_{y,n}$, $B_{y,n}$ and $C_{y,n}$ was achieved by Gehrmann *et al.* [14, 27]. In addition, $\overline{A}_{y,n}$, $\overline{B}_{y,n}$ and $\overline{C}_{y,n}$ are related to $A_{y,n}$, $B_{y,n}$ and $C_{y,n}$ according to

$$\begin{aligned} \overline{A}_{y,n} &= A_{y,n} , \\ \overline{B}_{y,n} &= B_{y,n} - \tfrac{3}{2}C_F A_{y,n} , \\ \overline{C}_{y,n} &= C_{y,n} - \tfrac{3}{2}C_F B_{y,n} + \left(\tfrac{9}{4}C_F^2 - K_2\right) A_{y,n} , \end{aligned} \quad (11)$$

The constant K_2 is given by [28, 29]

$$K_2 = \tfrac{1}{4}\left[-\tfrac{3}{2}C_F^2 + C_F C_A\left(\tfrac{123}{2} - 44\zeta_3\right) + C_F T_R N_F\left(-22+16\zeta_3\right)\right] , \quad (12)$$

where the QCD colour factors are

$$C_A = N , \qquad C_F = \frac{N^2-1}{2N} , \qquad T_R = \frac{1}{2} . \quad (13)$$

For $N=3$ colours and N_F light quark flavours. The coefficients A, B and C have been computed for several event-shape variables. In terms of the running coupling $\alpha_s\left(\mu^2\right)$, the NNLO expression for an event shape moment measured at centre-of-mass energy squared s becomes [14]

$$\begin{aligned} \langle y^n\rangle \left(s,\mu^2\right) &= \left(\frac{\alpha_s(\mu)}{2\pi}\right) \overline{A}_{y,n} + \left(\frac{\alpha_s(\mu)}{2\pi}\right)^2 \left(\overline{B}_{y,n} + \overline{A}_{y,n}\beta_0 \log\frac{\mu^2}{s}\right) \\ &+ \left(\frac{\alpha_s(\mu)}{2\pi}\right)^3 \left(\overline{C}_{y,n} + 2\overline{B}_{y,n}\beta_0\log\frac{\mu^2}{s} + \overline{A}_{y,n}\left(\beta_0^2\log^2\frac{\mu^2}{s} + \beta_1\log\frac{\mu^2}{s}\right)\right) \\ &+0\left(\alpha_s^4\right) \end{aligned} \quad (14)$$

in which

$$\begin{aligned} \beta_0 &= \frac{11C_A - 4T_R N_F}{6} , \\ \beta_1 &= \frac{17C_A^2 - 10C_A T_R N_F - 6C_F T_R N_F}{6} . \end{aligned} \quad (15)$$

3. Physics results

Moments of event shapes have been measured by various e^+e^- collider experiments at the centre-of-mass energies ranging from 40 GeV to 207 GeV [30, 31].

To determine α_s at each energy point, the measured distributions are fitted in the ranges of energies. In this paper, we use the experimental data for the five variables at $\langle\sqrt{s}\rangle = 200.2$ GeV. The scale uncertainly is obtained by repeating the fit for different values of the renormalization scale in the interval $0.5\sqrt{s} \leq \mu \leq 2\sqrt{s}$ [32].

The moments of the five standard event shapes are displayed in figures 1 and 2. The predictions are compared to L3 and DELPHI data. Our real data are consistent with NNLO, compared with NLO or LO calculations, because it involves higher order terms in QCD calculations [14].

The value of α_s was estimated by fitting the data [30, 31] with the NNLO expression for an event shape moment (14). Separate fits were performed to each of the five observables at the centre-of-mass energies ranging from 40 GeV to 207 GeV [30, 31]. The fitted values for α_s change for different choices of the renormalization scale. This is demonstrated for the moments of event shapes in Tables I–V. The given errors are statistical. We also have indicated on each table the value of $\alpha_s(M_Z)$ extracted at M_Z energy. We do not observe any significant change between the values of strong coupling constant for different event shape moments and renormalization scales.

TABLE I

Measurement of α_s from $\langle(B_T)\rangle$ and $\langle(B_T)^2\rangle$ moments for different choices of the renormalization scale.

Event shape variable	μ	α_s
$\langle(B_T)\rangle$	$\sqrt{s}/4$	0.1327 ± 0.0008
	M_Z	0.1268 ± 0.0008
	$\sqrt{s}/3$	0.1254 ± 0.0009
	$\sqrt{s}/2$	0.1188 ± 0.0009
	$\sqrt{s}$	0.1131 ± 0.0009
	$2\sqrt{s}$	0.1104 ± 0.0009
$\langle(B_T)^2\rangle$	$\sqrt{s}/4$	0.1345 ± 0.0022
	M_Z	0.1294 ± 0.0020
	$\sqrt{s}/3$	0.1285 ± 0.0021
	$\sqrt{s}/2$	0.1230 ± 0.0021
	$\sqrt{s}$	0.1182 ± 0.0021
	$2\sqrt{s}$	0.1159 ± 0.0020

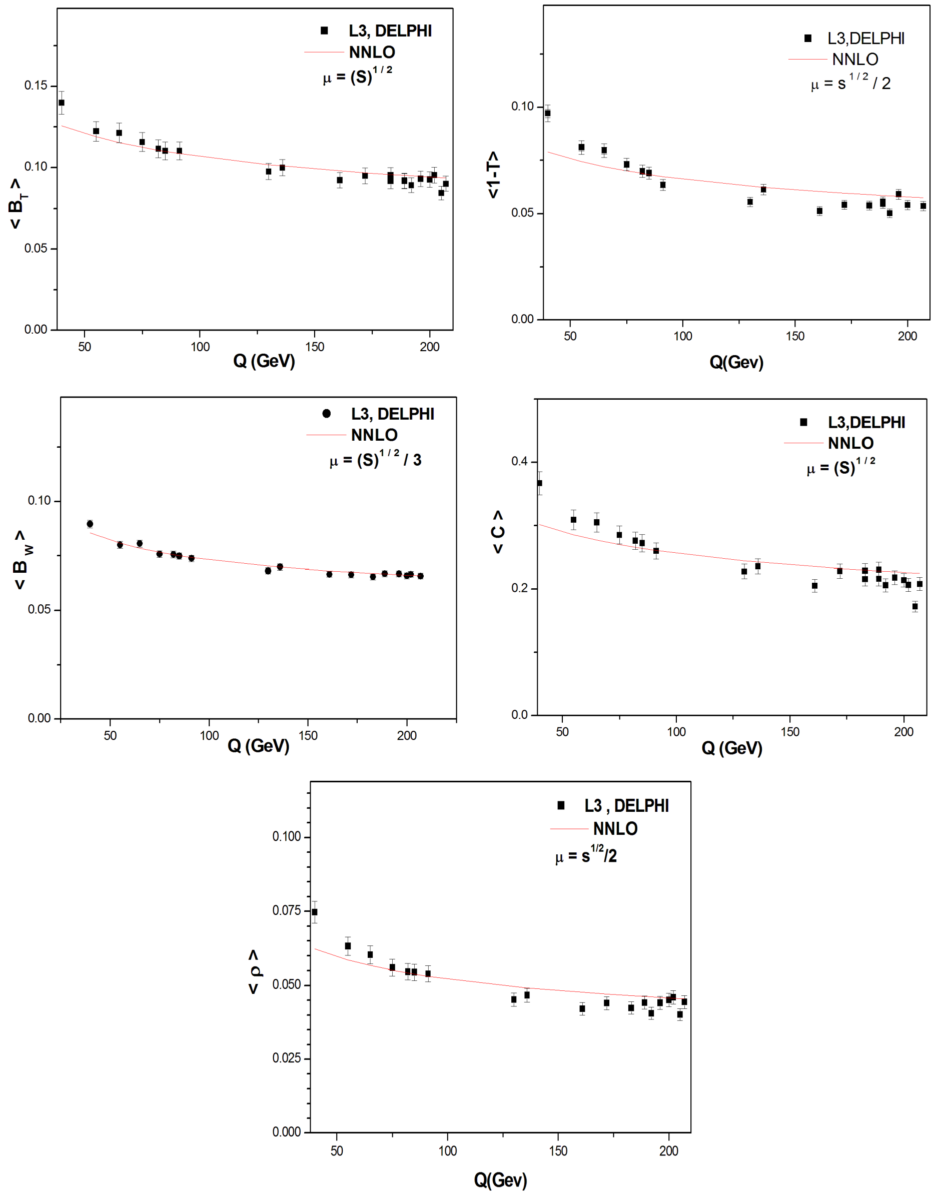

Fig. 1. First moments of five event shape variables fitted with Eq. (14). The data are from the L3 and DELPHI experiments, taken from Refs. [30, 31].

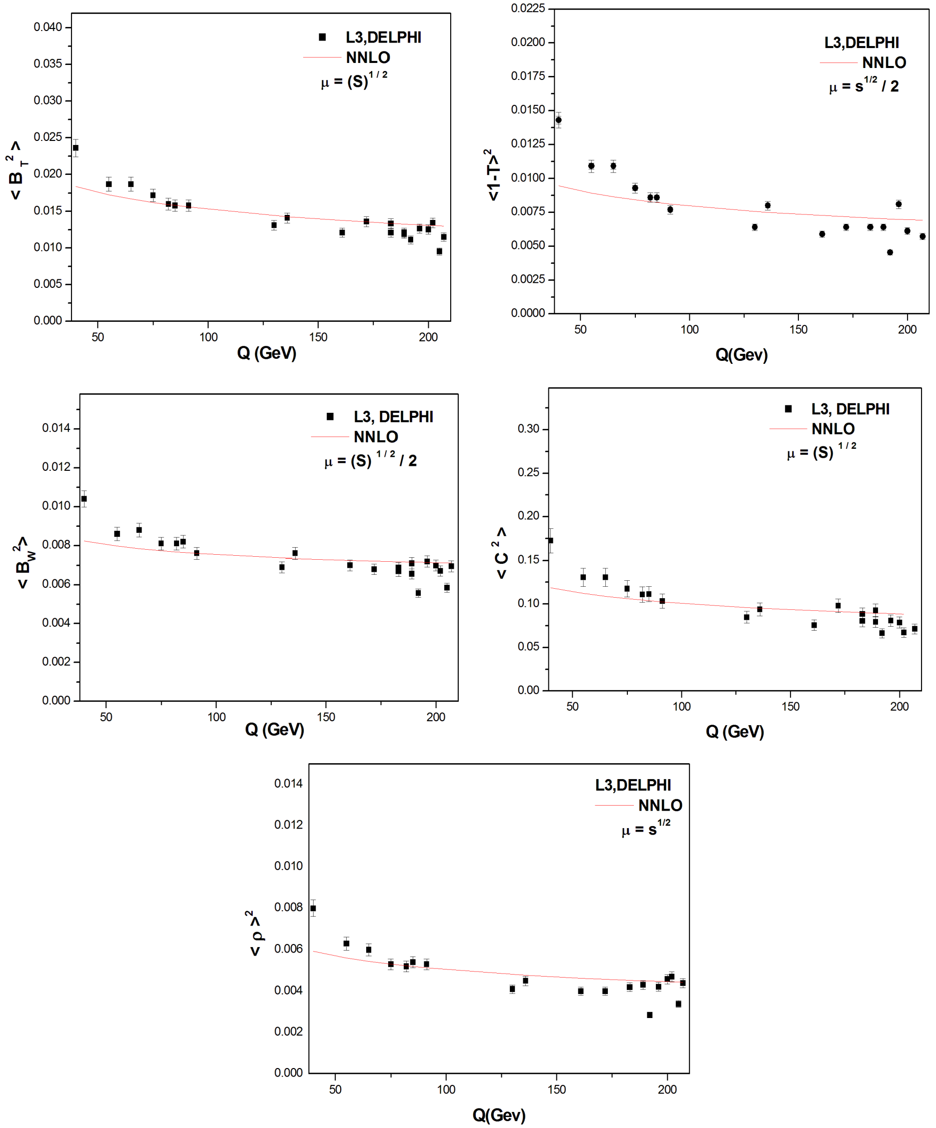

Fig. 2. Second moments of five event shape variables fitted with Eq. (14). The data are from the L3 and DELPHI experiments, taken from Refs. [30, 31].

TABLE II

Measurement of α_s from $\langle 1-T\rangle$ and $\langle (1-T)^2\rangle$ moments for different choices of the renormalization scale.

Event shape variable	μ	α_s
$\langle 1-T\rangle$	$\sqrt{s}/4$	0.1339 ± 0.0024
	M_Z	0.1298 ± 0.0021
	$\sqrt{s}/3$	0.1273 ± 0.0023
	$\sqrt{s}/2$	0.1211 ± 0.0022
	$\sqrt{s}$	0.1158 ± 0.0021
	$2\sqrt{s}$	0.1133 ± 0.0021
$\left\langle (1-T)^2\right\rangle$	$\sqrt{s}/4$	0.1377 ± 0.0049
	M_Z	0.1364 ± 0.0039
	$\sqrt{s}/3$	0.1316 ± 0.0047
	$\sqrt{s}/2$	0.1260 ± 0.0045
	$\sqrt{s}$	0.1210 ± 0.0043
	$2\sqrt{s}$	0.1186 ± 0.0042

TABLE III

Measurement of α_s from $\langle (B_W)\rangle$ and $\langle (B_W)^2\rangle$ moments for different choices of the renormalization scale.

Event shape variable	μ	α_s
$\langle (B_W)\rangle$	$\sqrt{s}/4$	0.1297 ± 0.0009
	M_Z	0.1249 ± 0.0006
	$\sqrt{s}/3$	0.1228 ± 0.0008
	$\sqrt{s}/2$	0.1159 ± 0.0007
	$\sqrt{s}$	0.1097 ± 0.0006
	$2\sqrt{s}$	0.1068 ± 0.0006
$\left\langle (B_W)^2\right\rangle$	$\sqrt{s}/4$	0.1231 ± 0.0016
	M_Z	0.1195 ± 0.0013
	$\sqrt{s}/3$	0.1166 ± 0.0015
	$\sqrt{s}/2$	0.1107 ± 0.0014
	$\sqrt{s}$	0.1055 ± 0.0014
	$2\sqrt{s}$	0.1031 ± 0.0013

TABLE IV

Measurement of α_s from $\langle C \rangle$ and $\langle C^2 \rangle$ moments for different choices of the renormalization scale.

Event shape variable	μ	α_s
$\langle C \rangle$	$\sqrt{s}/4$	0.1324 ± 0.0019
	M_Z	0.1272 ± 0.0017
	$\sqrt{s}/3$	0.1258 ± 0.0019
	$\sqrt{s}/2$	0.1197 ± 0.0018
	$\sqrt{s}$	0.1144 ± 0.0018
	$2\sqrt{s}$	0.1120 ± 0.0017
$\langle C^2 \rangle$	$\sqrt{s}/4$	0.1364 ± 0.0039
	M_Z	0.1335 ± 0.0029
	$\sqrt{s}/3$	0.1305 ± 0.0038
	$\sqrt{s}/2$	0.1249 ± 0.0036
	$\sqrt{s}$	0.1200 ± 0.0035
	$2\sqrt{s}$	0.1177 ± 0.0035

TABLE V

Measurement of α_s from $\langle \rho \rangle$ and $\langle \rho^2 \rangle$ moments for different choices of the renormalization scale.

Event shape variable	μ	α_s
$\langle \rho \rangle$	$\sqrt{s}/4$	0.1367 ± 0.0021
	M_Z	0.1304 ± 0.0020
	$\sqrt{s}/3$	0.1287 ± 0.0020
	$\sqrt{s}/2$	0.1215 ± 0.0019
	$\sqrt{s}$	0.1153 ± 0.0018
	$2\sqrt{s}$	0.1124 ± 0.0018
$\langle \rho^2 \rangle$	$\sqrt{s}/4$	0.1317 ± 0.0035
	M_Z	0.1260 ± 0.0033
	$\sqrt{s}/3$	0.1246 ± 0.0033
	$\sqrt{s}/2$	0.1180 ± 0.0030
	$\sqrt{s}$	0.1124 ± 0.0029
	$2\sqrt{s}$	0.1098 ± 0.0028

We observe that our obtained values for coupling constant considering the NNLO corrections for different event shape variables are in good agreement with the other experiments [10].

4. Conclusions

In this paper, we have presented measurements of the strong coupling constant for hadronic events produced at L3 and DELPHI in the centre-of-mass energies from 40 GeV to 207 GeV. We measured the coupling constant considering the moments of the event shape observables using NNLO calculations for different choices of the renormalization scale. Our results are consistent with those obtained from other experiments, as well as with the QCD theory.

REFERENCES

[1] V. Abazov *et al.* [D0 Collaboration], *Phys. Rev.* **D80**, 071102 (2009).

[2] A. Pak, M. Rogal, M. Steinhauser, *Phys. Lett.* **B679**, 473 (2009).

[3] T. Aaltonen *et al.*, *Phys. Rev.* **D80**, 051104 (2009).

[4] V. Abazov *et al.*, *Phys. Rev. Lett.* **103**, 132001 (2009).

[5] U. Langenfeld, S. Moch, P. Uwer, *Phys. Rev.* **D80**, 054009 (2009).

[6] R. Barate *et al.* [ALEPH Collaboration], *Eur. Phys. J.* **C18**, 1 (2000) [arXiv:hep-ex/0008013].

[7] G. Abbiendi *et al.* [OPAL Collaboration], *Eur. Phys. J.* **C21**, 411 (2001) [arXiv:hep-ex/0105046].

[8] G. Abbiendi *et al.* [JADE and OPAL collaborations], *Eur. Phys. J.* **C17**, 19 (2000).

[9] W. Bartel *et al.* [JADE Collaboration], *Z. Phys.* **C33**, 23 (1986).

[10] A. Gehrmann, T. Gehrmann, E.W.N. Glover, G. Heinrich, *J. High Energy Phys.* **0712**, 094 (2007).

[11] A. Gehrmann, T. Gehrmann, E.W.N. Glover, G. Heinrich, *PoS* **RAD COR**, 048 (2007).

[12] S. Weinzierl, *J. High Energy Phys.* **0906**, 041 (2009).

[13] M.E. Zomorrodian, A. Sepehri, A. Moradi Marjaneh, *Int. J. Phys.* **1**, 1 (2010).

[14] A. Gehrmann-De Ridder, T. Gehrmann, E.W.N. Glover, G. Heinrich, *J. High Energy Phys.* **0905**, 106 (2009).

[15] A. Gehrmann, T. Gehrmann, E.W.N. Glover, G. Heinrich, *J. High Energy Phys.* **0711**, 058 (2007).

[16] G. Dissertori *et al.*, *Nucl. Phys. Proc. Suppl.* **183**, 2 (2008).

[17] D.A. Kosower, *Phys. Rev.* **D57**, 5410 (1998).

[18] A. Daleo, T. Gehrmann, D. Maitre, *J. High Energy Phys.* **0704**, 016 (2007).

[19] A. Gehrmann-De Ridder, T. Gehrmann, E.W.N. Glover, *J. High Energy Phys.* **0509**, 056 (2005).

[20] A. Gehrmann-De Ridder, T. Gehrmann, E.W.N. Glover, G. Heinrich, *Phys. Rev. Lett.* **100**, 172001 (2008).

[21] A. Gehrmann-De Ridder, T. Gehrmann, E.W.N. Glover, G. Heinrich, *Phys. Rev. Lett.* **99**, 132002 (2007).

[22] S. Weinzierl, *J. High Energy Phys.* **0906**, 041 (2009).

[23] S. Weinzierl, *Phys. Rev. Lett.* **101**, 162001 (2008).

[24] S. Weinzierl, *J. High Energy Phys.* **0907**, 009 (2009).

[25] G. Dissertori *et al.*, *Nucl. Phys. Proc. Suppl.* **183**, 2 (2008).

[26] S. Catani, B.R. Webber, Y.L. Dokshitzer, F. Fiorani, *Nucl. Phys.* **B383**, 419 (1992).

[27] A. Gehrmann-De Ridder, T. Gehrmann, E.W.N. Glover, G. Heinrich, *J. High Energy Phys.* **0712**, 094 (2004).

[28] S. Catani, S. Dittmaier, Z. Trocsanyi, *Phys. Lett.* **B500**, 149 (2001) [`arXiv:hep-ph/0011222`].

[29] M. Cacciari, S. Catani, *Nucl. Phys.* **B617**, 253 (2001) [`arXiv:hep-ph/0107138`].

[30] S. Catani, S. Dittmaier, M.H. Seymour, Z. Trocsanyi, *Nucl. Phys.* **B627**, 189 (2002) [`arXiv:hep-ph/0201036`].

[31] M. Cacciari, E. Gardi, *Nucl. Phys.* **B664**, 299 (2003) [`arXiv:hep-ph/0301047`].

[32] L3 Collaboration, *Phys. Rep.* **399**, 71 (2004).